ACOUSTICS AND VIBRATIONS OF SANDWICH STRUCTURES – AN OVERVIEW

Steven Nutt, Changzheng Huang, Portia Peters, and Christina Naify

Gill Foundation Composites Center
University of Southern California, Los Angeles, CA 90089-0241, USA
nutt@usc.edu

ABSTRACT

This paper provides an overview of recent research on sandwich structure acoustics at the Gill Foundation Composites Center. Research is focused on three areas: (1) measuring the acoustic absorption and loss factors of honeycomb sandwich structures with a focus on the material impact; (2) exploiting impedance mismatch of gas layers to reduce sound transmission, and (3) numerical modeling of sound transmission through sandwich panels. Results from these activities are presented and discussed.

1. INTRODUCTION

With regard to the acoustics of sandwich structures, current research at USC Composites Center has focused on three main areas:

Loss factor measurement

Experiments have been performed to determine loss factors for honeycomb sandwich panels with composite face sheets [1-2], combining honeycomb and viscoelastic material to improve damping and limit vibration [3], and determining the effects of delamination on damping in honeycombs [4-6].

Noise control by impedance mismatch

Noise control is an important engineering problem for design of transportation vehicles, such as planes, trains, and automobiles. Gas layers can be an effective noise reduction measure, particularly in weight-critical structures such as aircraft and space vehicles, although there are few examples of practical implementation as yet. The underlying concept involves exploiting the impedance mismatch between gas layers.

Numerical modeling for sound transmission

The third aspect of the research involves the development of numerical prediction capabilities for sound transmission through sandwich panels. Sandwich panels are commonly used in airplane flooring and cabin structures. In these applications, a design requirement of increasing importance for sandwich panels is that they significantly reduce or block noise transmission from external sources such as engines and turbulent flow. Numerical predictions for sound transmission through sandwich panels have been studied extensively. Earlier studies are often based on reduced governing equations by making simplified assumptions about the sandwich panel deformations. With the increasing use of composite laminates in sandwich constructions, more complex numerical models based on higher-order theory or even full elasticity equations are required. Our recent research effort has focused on developing numerical prediction capability based on 3-D elasticity theory. Below we describe the three research areas in detail.

2. LOSS FACTOR

2.1 Experimental setup

Oberst beam method. The classical method for measuring damping characteristics of materials is the Oberst beam method. Problems with the effects of clamping conditions on the dynamic characteristics of composite cantilever beams were investigated by Hwang et al [7], who attempted to increase the natural frequency and damping of structures. These clamping condition limitations prompted the search for an excitation method that did not interfere with the data collection. This led to consideration of the free-free configuration. Damping measurements using this configuration were performed on five honeycomb sandwich beams, listed in Table 1. The sample names correspond to the panels used by Rajaram et al [8].

Table 1. List of beams tested and their properties.

Sample Name	Skin Type	Core Material	Special Properties
G	Glass/Epoxy	Nomex®	
H	Glass/Epoxy	Kevlar®	
C	Carbon	Nomex®	
MP	Carbon	Nomex®	Mid-plane damping layer
SSS-2	Carbon	Nomex®	Subsonic core

Suspended beam method. The suspended beam method was used for the sandwich beam with a viscoelastic layer inserted at the midplane (Sample MP). This method was validated by first testing a lightly damped beam to confirm that the first few modes were accurately measured. After this, the predicted resonant frequencies of the beam were calculated and compared against the experimental resonant frequencies, confirming the accuracy. The surface velocity was measured at one centimeter increments along the beam. This differs from the Oberst beam method because the loss factor was calculated using the measured damping ratio (as opposed to the velocity). This difference is a consequence of the two testing methods and did not affect the measured loss factor values.

2.2 Loss factor results

Mid-plane damping. These samples featured a viscoelastic sheet inserted at the mid-plane of the honeycomb core to increase damping. The mid-plane coincides with the maximum shear force in the beam when a bending load is applied. The effect of the damping layer was assessed by comparing the damping properties with a conventional sandwich beam featuring identical skin and core materials (sample C). The mid-plane damping layer increased the loss factor of the beam by up to 233%. Fig. 1 also shows that the damping curve for sample MP is parallel to the control panel C over the entire frequency spectrum, demonstrating that the damping from the mid-plane viscoelastic layer is independent of frequency. This behavior indicates that the operative damping mechanism is unlike constrained layer damping (CLD), which is usually frequency dependent, while free layer damping is not.

Skin damping. Comparison of samples G and C revealed the effect of skin material on damping. Sample G featured glass/epoxy face sheets, while sample C featured carbon face sheets. Sample C showed a consistently higher loss factor than panel G over the

entire frequency range. However, it is commonly accepted that glass fiber composites exhibit higher damping factors than carbon fiber laminates. The apparent contradiction shown here can be attributed to two possible causes. First, the fibers used in the construction of the panel as well as the fiber treatment and type of adhesives used in the sandwich panel can affect the measured loss factor. In other studies of noise mitigation factors (i.e. transmission loss), details such as these are minor relative to the overwhelming structural effects. However, in loss factor measurements, material properties play a more significant role. Second, the material structure of the carbon skin could be responsible for the higher loss factor than the glass-epoxy skin. The turbostratic structure of carbon fibers features well-aligned basal planes which are only weakly bonded, allowing for interplanar sliding. Similar enhanced damping is observed in other C-based structures, such as carbon nanotube-reinforced epoxies, and certain cast irons containing graphitic flakes

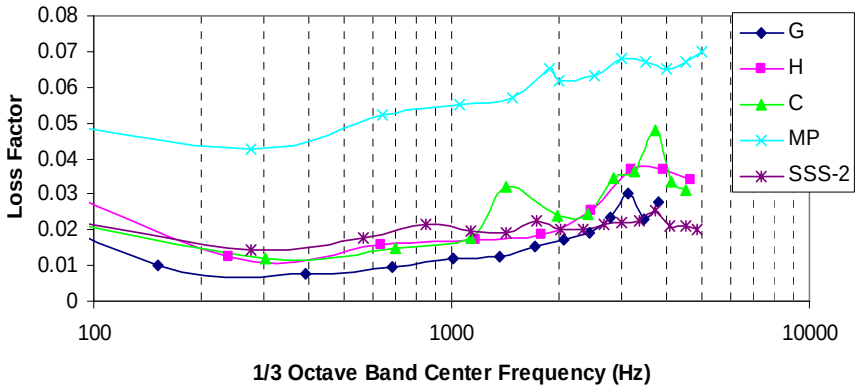

Figure 1. Loss factor values for the five composite sandwich beam samples

Wave speed. Sample SSS-2 featured a thinner core and thicker face sheets than conventional sandwich designs. This unconventional design was selected to achieve a subsonic shear wave speed of approximately two-thirds the speed of sound. Testing the subsonic panel for loss factor was an extension of previous work [8-9] that showed subsonic cores can increase the transmission loss of a panel by several decibels. A subsonic core increases the coincidence frequency and should thus, in principle, impart superior acoustical performance. However, the subsonic panel exhibited a lower loss factor than the control panel. This finding can be understood by noting that wave speed and damping are distinct parameters and do not necessarily follow similar trends.

Core materials. Sample H featured a para-aramid (Kevlar®) core, which was stiffer and stronger than conventional core materials. This panel yielded loss factor values that were greater than those of reference sample G, which featured a conventional meta-aramid (Nomex®) core (Fig. 1) particularly beyond 3 KHz. The difference in the loss factors stems from the different inherent stiffness of the meta- and para-aramid cores. The higher stiffness of Sample H arises from the use of para-aramid fiber paper, as opposed to meta-aramid fiber paper. In the sandwich structure, the stiffer para-aramid cores impart a lower modal density to the panel beyond the coincidence frequency, compared to meta-aramid cores of similar density [8-13]. This lower modal density enhances the panel damping [8]. The magnitude of the increase is comparable to the difference in mechanical properties of the constituent materials, because the para-aramid structure is molecularly aligned and gives imparts greater strength than the meta-aramid structure.

3. IMPEDANCE MISMATCH

3.1 Background

Sound waves traveling across the interface between different media experience inefficient transfer of energy [14-18]. The acoustic impedance of a gas (Z) is directly proportional to both the density of the gas (ρ) and the speed of sound through the gas (c). The impedance value is also related to the angle of incidence (θ) of the sound wave on the panel [19]. Some typical values of impedance for various gasses are presented in Table 2. The impedance mismatch between helium and air is large, resulting in an increase in transmission loss as sound waves pass from one gas to the other.

Table 2. Characteristic impedance for various gases.

Gas	Density (kg/m^3)	Speed of sound (m/s)	Impedance (kg/m^2s)
Air	1.23	341.4	419.9
Nitrogen	1.19	347.5	411.8
Argon	1.78	310	552.7
Helium	0.17	996.7	169.2

Once the impedance of each layer is determined, the transmission coefficient of the system can be calculated. The transmission coefficient (T) represents the ratio of the amplitudes of the transmitted and incident waves,

$$T = \frac{2Z_2 \cos\theta}{Z_2 \cos\theta + \rho c} = \frac{2Z_2}{Z_2 + Z_1} \tag{1}$$

In the case of normal incidence (θ=0) onto the panel, the value Z is the characteristic impedance. For large panels, sound transmission loss is generally larger for a normal incidence than for diffuse or random incidence [20]. Transmission loss (TL) is then calculated via the transmission coefficient. This value is normally measured in dB.

$$TL = 10 \log \frac{1}{|T|^2} \tag{2}$$

Transmission loss is generally used as a measure of effectiveness of sound attenuating measures.

3.2 Experimental setup

The TL test facility used to measure the transmission loss of the panels was a small-scale facility constructed in accordance with ASTM 2249-02 [19]. The facility consisted of source and receiver rooms separated by a window opening to hold the test panel. The test facility was calibrated between 315Hz and 10 kHz. The panel used to perform the tests was 1.067m x 1.067m. The panel was a sandwich structure with polyamide honeycomb core and carbon fiber face sheets (MC Gill Panel 15). The total thickness of the panel was 0.93cm. Data was collected at 121 evenly spaced points over the panel to obtain discreet sound measurements. Recorded intensity values were averaged over these points. The frequency range of the source was 100Hz to 10 kHz. Average sound source pressure levels were maintained at 90dB for all tests.

The gas layers used in the study were air, helium and argon. Constant pressure was maintained by regulating the gas content in each bladder and by using gas impermeable plastic films to construct the bladders. These film materials also were minimal in weight and did not increase the transmission loss of the system. All tests were conducted at room temperature

Gas was introduced into the bags using vacuum port nozzles and constant pressure was maintained for several hours. For the layered gas experiments, a double bag system was constructed using three sheets of the polymer film sealed at the edges. The gas was then introduced into each compartment with separate nozzles. The maximum thickness of the inflated bags averaged 70-90 mm in the center of the panel with diminished thickness along the bag periphery. Bags were evacuated before introducing the test gas.

3.3 Results of impedance mismatch

Application of layered gases to composite sandwich panels showed significant increases in transmission loss compared to the same panels alone [17]. The increase in transmission loss was greater for helium layers than for argon. When multiple gas layers were employed using different gases, the resulting TL values were greater than for any single gas layer tested. Table 3 shows the gasses used in the experimental study and the locations of the gas layers. Layering the gasses on the source side of the panel caused an increase in TL of a few dB at high frequencies and little or no increase at low to mid frequencies. This increase was more pronounced than the increase in TL observed from pure helium on the source side of the panel. The layered gasses, helium and argon, were held at constant pressure and mixing prevented by the use of the metalized polymer material.

Table 3. Location of tested gases.

No.	Tested gas	Location
1	Helium	Source side
2	Helium	Receiver side
3	Helium and Argon	Receiver side
4	Helium	Receiver side

Addition of gas layers to both source and receiver side of the panel produced the largest increase in TL. In particular, the addition of helium layers to both sides of the panel yielded a much larger TL increase than placing gas layers on either side of the panel alone. This increase is shown in Fig. 2. Over the frequency range of 1-10 KHz, the increase in TL was 13-17dB. The TL values at lower frequencies also increased more than previously demonstrated by single gas layers, with increases of 4-6 dB between 400 and 1000 Hz. All of the results obtained were repeatable over multiple trials. Transmission loss increase with the addition of helium to the source side, and helium and argon to the receiver side of the panel produced the largest overall increase at high frequencies.

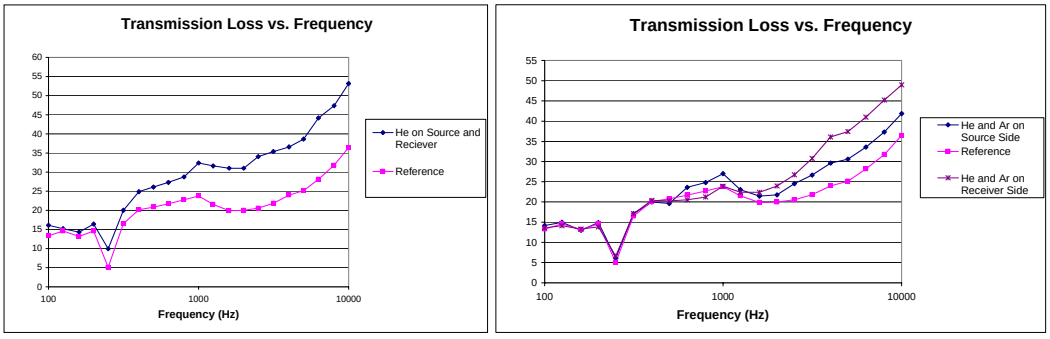

Figure 2. Transmission loss vs. frequency with gas layers.

4. SOUND TRANSMISSION MODELING

4.1 Sound transmission coefficient

Sound transmission through sandwich panels has been studied extensively [21-28]. In this section, we develop an analytical formulation for sound transmission through multi-layered panels based on the approach of 3-D elasticity theory [29-30]. Figure 3 shows a schematic diagram of an incident acoustic wave transmitted through a structural panel.

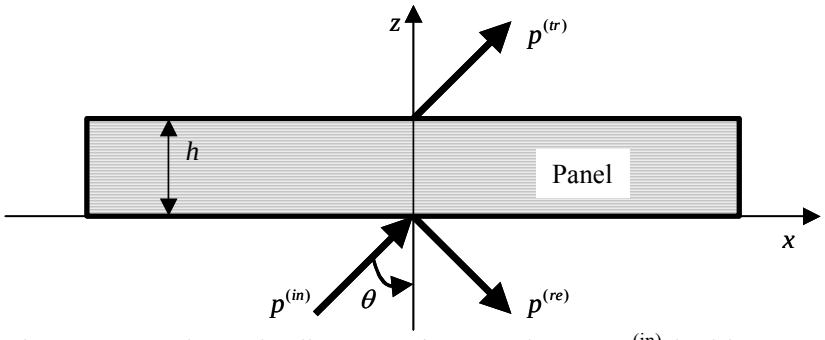

Figure 3. A schematic diagram of a sound wave $p^{(\mathrm{in})}$ incident on a panel of thickness h from the bottom surface with an incident angle θ. The reflected and transmitted waves are denoted as $p^{(\mathrm{re})}$ and $p^{(\mathrm{tr})}$, respectively. The incident wave lies in the xz-plane, which has the azimuthal angle ϕ=0.

The vibration of the panel is governed by the 3-D elasticity equations,

$$\begin{aligned}
&\frac{\partial \sigma_{xx}}{\partial x}+\frac{\partial \sigma_{yx}}{\partial y}+\frac{\partial \sigma_{zx}}{\partial z}=\rho\frac{\partial^2 u}{\partial t^2}\\
&\frac{\partial \sigma_{xy}}{\partial x}+\frac{\partial \sigma_{yy}}{\partial y}+\frac{\partial \sigma_{zy}}{\partial z}=\rho\frac{\partial^2 v}{\partial t^2}\\
&\frac{\partial \sigma_{xz}}{\partial x}+\frac{\partial \sigma_{yz}}{\partial y}+\frac{\partial \sigma_{zz}}{\partial z}=\rho\frac{\partial^2 w}{\partial t^2}
\end{aligned}. \tag{3}$$

Here ρ is the density of the panel, and

$$\begin{aligned}
&\mathbf{u}=\left(u,v,w\right)^T\\
&\boldsymbol{\sigma}=\left(\sigma_{xx},\sigma_{yy},\sigma_{zz},\sigma_{yz},\sigma_{zx},\sigma_{xy}\right)^T
\end{aligned} \tag{4}$$

are column vectors of displacements and stresses, respectively. The general stress-strain relationship reads,

$$\begin{pmatrix}\sigma_{xx}\\ \sigma_{yy}\\ \sigma_{zz}\\ \sigma_{yz}\\ \sigma_{zx}\\ \sigma_{xy}\end{pmatrix}=\begin{pmatrix}C_{11}&C_{12}&C_{13}&C_{14}&C_{15}&C_{16}\\ C_{21}&C_{22}&C_{23}&C_{24}&C_{25}&C_{26}\\ C_{31}&C_{32}&C_{33}&C_{34}&C_{35}&C_{36}\\ C_{41}&C_{42}&C_{43}&C_{44}&C_{45}&C_{46}\\ C_{51}&C_{52}&C_{53}&C_{54}&C_{55}&C_{56}\\ C_{61}&C_{62}&C_{63}&C_{64}&C_{65}&C_{66}\end{pmatrix}\begin{pmatrix}\partial u/\partial x\\ \partial v/\partial y\\ \partial w/\partial z\\ \partial w/\partial y+\partial v/\partial z\\ \partial u/\partial z+\partial w/\partial x\\ \partial v/\partial x+\partial u/\partial y\end{pmatrix}. \tag{5}$$

Because the panel extends to infinity, the appropriate solution has the following form,

$$\begin{aligned}\mathbf{u}(x,y,z,t) &= \hat{\mathbf{u}}(z)e^{ik_x x}e^{ik_y y}e^{-i\omega t}\\ \boldsymbol{\sigma}(x,y,z,t) &= \hat{\boldsymbol{\sigma}}(z)e^{ik_x x}e^{ik_y y}e^{-i\omega t}\end{aligned}. \tag{6}$$

Here ω is the circular frequency, and k_x and k_y are two in-plane wave numbers. From the equations above, a transfer matrix can be derived that relates the displacement and z-component stresses on the top surface to those on the bottom surface [30], i.e.,

$$\begin{pmatrix}\hat{u}^{(top)}\\ \hat{v}^{(top)}\\ \hat{w}^{(top)}\\ \hat{\sigma}_{zx}^{(top)}\\ \hat{\sigma}_{zy}^{(top)}\\ \hat{\sigma}_{zz}^{(top)}\end{pmatrix} = \begin{pmatrix}t_{11} & t_{12} & t_{13} & t_{14} & t_{15} & t_{16}\\ t_{21} & t_{22} & t_{23} & t_{24} & t_{25} & t_{26}\\ t_{31} & t_{32} & t_{33} & t_{34} & t_{35} & t_{36}\\ t_{41} & t_{42} & t_{43} & t_{44} & t_{45} & t_{46}\\ t_{51} & t_{52} & t_{53} & t_{54} & t_{55} & t_{56}\\ t_{61} & t_{62} & t_{63} & t_{64} & t_{65} & t_{66}\end{pmatrix}\begin{pmatrix}\hat{u}^{(bot)}\\ \hat{v}^{(bot)}\\ \hat{w}^{(bot)}\\ \hat{\sigma}_{zx}^{(bot)}\\ \hat{\sigma}_{zy}^{(bot)}\\ \hat{\sigma}_{zz}^{(bot)}\end{pmatrix} = \mathbf{T}\begin{pmatrix}\hat{u}^{(bot)}\\ \hat{v}^{(bot)}\\ \hat{w}^{(bot)}\\ \hat{\sigma}_{zx}^{(bot)}\\ \hat{\sigma}_{zy}^{(bot)}\\ \hat{\sigma}_{zz}^{(bot)}\end{pmatrix} \tag{7}$$

Here the superscript *Top* stands for the top panel surface, and the superscript *Bot* stands for the bottom panel surface. The method for obtaining the exact expressions for the transfer matrix is given in Ref. [30]. With further manipulation, the sound transmission and reflection coefficients are,

$$\tau = \left|\frac{-2N\rho_0 c_0\omega\cos\theta}{-M_1\cos^2\theta + (M_2+M_3)i\rho_0 c_0\omega\cos\theta + M_4(\rho_0 c_0\omega)^2}\right|^2 \tag{8}$$

$$r = \left|\frac{-M_1\cos^2\theta + (M_2-M_3)i\rho_0 c_0\omega\cos\theta - M_4(\rho_0 c_0\omega)^2}{-M_1\cos^2\theta + (M_2+M_3)i\rho_0 c_0\omega\cos\theta + M_4(\rho_0 c_0\omega)^2}\right|^2 \tag{9}$$

Here, ρ_0 and c_0 are density and speed of sound of the ambient acoustic medium. The exact expressions for N, M_1 through M_4 are given in Ref. [30]. Equations (8) and (9) are the central results of this study. They represent the exact analytical solutions of the acoustic transmission and reflection coefficients for general panels. For multi-layered panels, the transfer matrix is the product of all the component transfer matrices. The solutions from this 3-D elasticity model can be used to study sound transmission characteristics for general multi-layered panels, including sandwich panels.

4.2 Numerical result

We consider a benchmark test example. The example is taken from Moore and Lyon [24]. The sandwich panel has two 6.35mm (¼-in) plywood face sheets and a 76.2mm (3-in) styrofoam core. For modeling purposes, both the face layers and core layer are assumed to be isotropic. The core properties are: density ρ=16 kg/m^3, Young's modulus E=12.5 MPa, and shear modulus G=3.1 MPa. The face layer properties are: Young's modulus E=7 GPa, area density m=3.73 kg/m3, and Poisson's ratio μ=0.38.

The sound transmission predictions from the 3-D elasticity theory are shown in Fig. 4. For comparison, the results from the Moore-Lyon method and the experimental data are also displayed in Fig. 4. The first large dip near 1.2 KHz in the numerical results marks the critical coincident frequency. Both the 3-D elasticity model and the Moore-Lyon method predict this coincident frequency accurately. The agreement between the model prediction and the experimental data is apparent up to a frequency of about 3 KHz. The discrepancies beyond that point are notable and may be caused by multiple effects. In

the modeling, the panel was assumed to be infinitely large and the acoustic damping was not considered. These two factors differ from the real case, in which the acoustic damping might be significant at higher frequencies and the panel size is always finite. Nevertheless, the numerical results demonstrate the superior prediction performance of the 3-D elasticity model for low to medium frequencies.

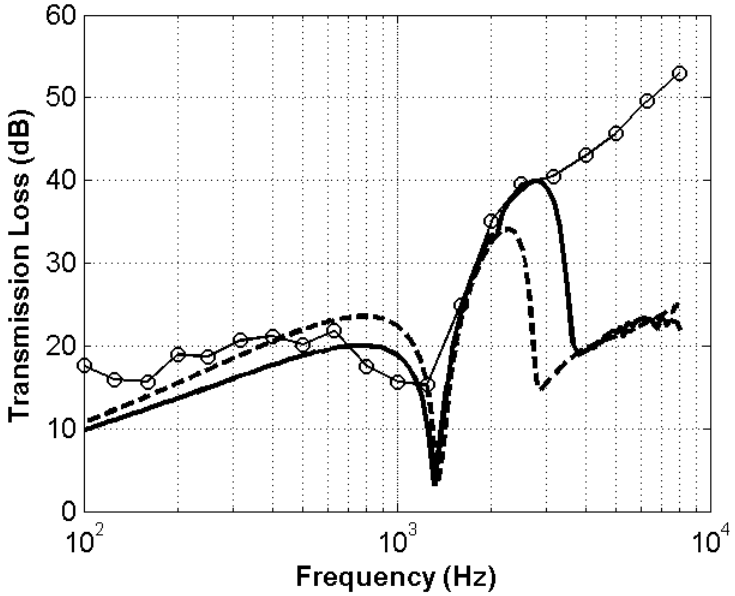

Figure 4. A comparison of sound transmission loss for the sandwich panel example: prediction from the 3-D elasticity theory (solid thick line), prediction from the Moore-Lyon method (dashed thick line), and data from experimental measurement (thin line with circles).

5. CONCLUSIONS

From a materials perspective, noise control of sandwich panels can be strongly influenced by both additive materials, such as the mid-plane viscoelastic material, and by the particular choice of skin materials. While the mid-plane damping layer and the para-aramid core increased the loss factor, the subsonic core did not. However, in past work the subsonic core resulted in substantially increased transmission loss. Inserting the mid-plane layer demonstrated the potential of judiciously placed damping materials. This approach could be extended to applications such as automotive frames and panels and airplane fuselages. While the focus of the present work was on frequencies above the coincidence frequency, increased damping at lower frequencies is expected to reduce transmission loss in this mass-controlled frequency range.

Overall, noise control requires a comprehensive perspective and solutions that encompass both transmission loss and damping. The present study confirms that the acoustical performance of sandwich structures is influenced by a variety of components that are independently linked. Weight penalties must also be considered when designing acoustically superior panels as a component that improves the loss factor could easily decrease the mechanical efficiency of the sandwich structure. Investigating materials and their combination of properties can also be manipulated to produce the optimal structure for aerospace applications.

We have also developed a numerical model for sound transmission. The 3-D elasticity theory based analytical solution is important and useful in analyzing sound transmission characteristics of sandwich panels. It can also be used in reverse as a design tool to design sandwich constructions to meet pre-specified sound transmission requirement. The 3-D model can be extended to include materials damping and panel size effect. Our current work is focused on applying the 3-D elasticity model to study the sound transmission through panels of functionally graded materials (FGM).

ACKNOWLEDGEMENTS
The authors are grateful for financial support from the Merwyn C. Gill Foundation.

REFERENCES

1- Peters P., Sneddon M., Nutt S. "Loss factors of honeycomb sandwich structures, an experimental approach", *Proceedings of the Institute of Noise Control Engineering of USA*, Reno, Nevada, 2007.
2- Renji K., Narayan S., "Loss factors of composite honeycomb sandwich panels", *Journal of Sound and Vibration*, 2002;250(4):745-761.
3- Jung W. Y., Aref A. J., "A combined honeycomb and solid viscoelastic material for structural damping applications", *Mechanics of Materials*, 2003;35:831-844.
4- Li Z., Crocker M. J., "Effects of thickness and delamination on the damping in honeycomb-foam sandwich beams", *Journal of Sound and Vibration*, 2006;294:473-485.
5- Shi Y., Sol H., Hua H., "Material parameter identification of sandwich beams by an inverse method", *Journal of Sound and Vibration*, 2006;290:1234-1255.
6- Wojtowicki J. L., Jaouen L., Panneton R., "A new approach for the measurement of damping properties of materials using the Oberst beam", *Review of Scientific Instruments*, 2004;75(8):2569-2574.
7- Hwang H. Y., Hak G. L., Lee D. G., "Clamping effects on the dynamic characteristics of composite machine tool structures", *Composite Structures*, 2004;66:399-407.
8- Rajaram S., Peters P., Wang T., Nutt S., "Comparison of acoustical performance of Kevlar vs Nomex honeycomb cores in sandwich panels", *Proceedings of the Society for the Advancement of Material and Process Engineering* (2006)
9- Rajaram S., Wang T., Chui Y., Allen G., Thirunarayanan P., Nutt S., "Measurement and prediction of sound transmission loss for airplane floors", *Proceedings of the American Institute of Aeronautics and Astronautics*, (2005).
10- Cremer, Heckl, Ungar, *Structure-Borne Sound 2nd edition*, Springer-Verlag, Berlin, Germany, (1987)
11- Bitzer T., *Honeycomb Technology,* Chapman & Hall, London, England, (1997)
12- Kyriazoglou C., Guild F. J., "Finite element prediction of damping of composite GFRP and CFRP laminates – a hybrid formulation – vibration damping experiments and Rayleigh damping", *Composites Science and Technology*, 2006;66:487-498.
13- Paolozzi A., I. Peroni I., "Response of aerospace sandwich panels to launch acoustic environment", *Journal of Sound and Vibration*,1996;196(1):1-18.
14- Atwal M. S., Crocker M. J., "The effect on the transmission loss of a double wall panel of using helium gas in the gap", *Proceedings of the National Conference on Noise Control Engineering*, Columbus, OH, 1985:187-192.

15- Raju P. K., Crocker M. J., "Prediction of Sound Transmission Through Double Walled Systems Containing Helium", *Journal of the Acoustical Society of America*, 1985;78:S59.
16- Belvins J. G., Hansen L. L., "Use of helium gas to reduce acoustic transmission", AIAA A85-30330, *Proceedings of Structures, Structural Dynamics, and Materials Conference*, 26th Orlando, FL, April 15-17, (1985)
17- Rajaram S., Nutt S., "Measurement of sound transmission losses of honeycomb partitions with added gas layers", *Noise Control Engineering Journal* 2006;54(2):101-105.
18- Mohanty A. K., Oliver C. C., Purdy K. R., "Acoustic measurements in low-density gases", *J. Phys D: Appl. Phys.*, 1975;8:1198-1201.
19- Brekhovskikh L. M., Godin O. A., *Acoustics of Layered Media 1: Plane and Quasi-Plane Waves*, Springer-Verlag, Berlin Heidelberg 1990.
20- Beranek L. L., Ver I. L., *Noise and Vibration Control Engineering*, John Wiley and Sons, United States 1992.
21- Ford R. D., Lord P., Walker A. W., "Sound transmission through sandwich constructions", *Journal of Sound and Vibration*, 1967;5:9-21.
22- Narayanan S., Shanbhag R. L., "Sound transmission through a damped sandwich panel", *Journal of Sound and Vibration*, 1982;80:315-27.
23- Dym C. L., Lang D. C., "Transmission loss of damped asymmetric sandwich panels with orthotropic cores", *Journal of Sound and Vibration*, 1983;88:299-319.
24- Moore J. A., Lyon R. H., "Sound transmission loss characteristics of sandwich panel constructions", *Journal of Acoustical Society of America*, 1991;89:777-91.
25- Wang T., Sokolinsky V. S., Rajaram S., Nutt S. R., "Assessment of sandwich models for the prediction of sound transmission loss in unidirectional sandwich panels", *Applied Acoustics*, 2005; 66:245-62.
26- Liang C., Rogers C. A., Fuller C. R., "Acoustic transmission and radiation analysis of adaptive shape memory alloy reinforced laminated plates", *Journal of Sound and Vibration*, 1991;145:23-41.
27- Kuo Y. M., Lin H. J., Wang C. N., "Sound transmission across orthotropic laminates with a 3D mode", *Applied Acoustics*, 2007; doi: 10.1016/j.apacoust. 2007.08.002.
28- Cai C., Liu G. R., Lam K. Y., "An exact method for analyzing sound reflection and transmission by anisotropic laminates submerged in fluids", *Applied Acoustics*, 2000;61:95-109.
29- Huang C., Nutt S., "Noise reduction study of sandwich plates using the state space method", *Proceedings of the Institute of Noise Control Engineering of USA*, Reno, Nevada, 2007.
30- Huang C., Nutt S., "Sound transmission prediction by 3-D elasticity theory", (Under review by *Applied Acoustics*).